J Sign Process Syst (2012) 68:247–259
DOI 10.1007/s11265-011-0609-7

Optimization Design of Biorthogonal Wavelet Filter Banks for Extending JPEG 2000 Standard Part-2

Guoan Yang · Huub Van de Wetering · Songjun Zhang

Received: 19 December 2009 / Revised: 13 July 2011 / Accepted: 13 July 2011 / Published online: 5 August 2011

Abstract A generic optimization design approach of biorthogonal wavelet filter banks (BWFB) for extending the JPEG 2000 standard part-2 is presented in this paper. This approach adopts Vaidyanathan optimal coding gain criterion to design the BWFB, and adopts peak signal-to-noise ratio (PSNR) as the criterion to optimize this BWFB. A functional relation between the general BWFB and their lifting scheme is derived in the first place with respect to one free variable, so that the optimization design of the BWFB is easier and more convenient. In addition, a general image model is formulated as a first-order Markov process driven by Gaussian white noise. It is taken as an input of two-channel filter banks which satisfy perfect reconstruction (PR) condition to realize subband coding for obtaining the optimal BWFB according to the Vaidyanathan optimal coding gain criterion. Finally, a new 9/7 BWFB with rational coefficients is proposed for extending the JPEG 2000 standard part-2, with PSNR of reconstructed images only 0.20 dB lower than standard CDF 9/7 BWFB for infrared thermal image compressions.

G. Yang (✉)
Institute of Artificial Intelligence and Robotics,
Xi'an Jiaotong University,
Xi'an 710049, China
e-mail: gayang@mail.xjtu.edu.cn

H. Van de Wetering
The Department of Mathematics and Computer Science,
Technische Universiteit Eindhoven,
Eindhoven, The Netherlands
e-mail: h.v.d.wetering@tue.nl

S. Zhang
Computing Mathematics, Xi'an Jiaotong University,
Xi'an 710049, China
e-mail: youyi000@gmail.com

Keywords Biorthogonal wavelet filter banks · Optimization design · Image compression · JPEG2000 standard part-2 · Lifting scheme

1 Introduction

The discrete wavelet transform (DWT) is widely known as to feature excellent decorrelation properties [1]. The DWT exhibits excellent lossy and lossless compression performance, and has been selected for the new standard JPEG2000 [2, 3]. The DWT based on lifting scheme [4–6] is realized by using the biorthogonal wavelet filter banks (BWFB) [7] and gives several excellent BWFB such as 9/7, 5/3 and 7/5 in the JPEG2000 standard part-1 and part-2. However, these BWFBs in the JPEG2000 standard part-1 and part-2 is surely not optimal to a certain type of image such as the texture image, remote sensing image, SAR image and so on. Therefore, it is expected that can quickly design an optimal BWFB to a type of image compression application for extending the JEPG2000 standard part-2. The optimization design of a BWFB for the JPEG2000 standard part-2 is a crucial task, and ingenious design enables superior quality for a broad class of images in computer applications and superior VLSI hardware implementations.

In order to obtain excellent image compression performances, the wavelet filters for the JEPG2000 standard are required to satisfy the compactly supported, perfect reconstruction (PR) condition, biorthogonal property, higher regularity and vanishing property, and linear phase etc. The efficiency of the BWFB in JPEG2000 image compression depends on the coefficients and length of filters and their lifting implementation structure. The BWFB has the best performance among various types of the wavelet filter banks for image compression. Generally speaking, the

optimization design approaches of the BWFB for the JPEG2000 standard part-2 can be classified into two categories. One category only considers the wavelet properties based on certain criteria such as the coding gain criterion, regularity criterion, rate distortion criterion and energy compaction criterion. The other category is based on the peak signal-to-noise ratio (PSNR) criterion of reconstructed images. So far, many approaches have been proposed to design the optimal BWFB for image compression, but hardly any work on the optimization design of the BWFB for the JPEG2000 standard part-2 has been published. Recently, theoretical approaches on design optimization of two channel BWFB were developed, for example, cyclostationary spectral analysis of Ohno [8], optimal biorthogonal filter banks of Vaidyanathan [9], optimal choice of a wavelet of Tewfik [10], least squares design of Tay [11], and optimization design using rate distortion criterion of Moulin [12]; furthermore, Liu [13] presented a design method of the BWFB based on trigonometric polynomial depending on two free parameters, and Guo [14] proposes a filter design framework based on the CDF 9/7 filter, which employs chaos evolution programming to optimize the wavelet filter through only one tuning parameter for extending the JPEG2000 wavelet kernels, but these approaches are not optimization designs based on the PSNR criterion. In this paper, we focus on the design and optimization of the arbitrary BWFB for the JPEG2000 standard part-2. Therefore, we present a new approach to quickly design and optimize the BWFB, where all coefficients of the BWFB and their lifting parameters are rational numbers, resulting in a DWT with low computational complexity and high suitability for VLSI hardware implementation.

This paper is organized as follows. In section 2, we derive a generic JPEG2000 wavelet kernel and a one dimensional functional relation with respect to the BWFB and their lifting scheme implementation. In section 3, we introduce the basic assumptions of our image model, a namely first-order Markov model, it is used for theoretical design of the BWFB. In section 4, we propose our design approach of the BWFB by using this image model. In section 5, we provide a design example for the optimal 9/7 BWFB with rational coefficients based on JPEG2000 image compression criterion suitable for infrared thermal images, such that it can be used as a new wavelet kernel for the JPEG2000 standard part-2. Finally, in section 6, we discuss the conclusion and future work.

2 Generic JPEG2000 Wavelet Kernels

2.1 JPEG2000 Image Compression Systems

The JPEG 2000 standard employs the DWT based on a lifting scheme for image compression, it supports, among others, LeGall 5/3 BWFB for lossless compression, and the CDF 9/7 BWFB of Cohen, Daubechies and Feauveau and BT 7/5 of Brislawn and Treiber for lossy compression. The JPEG2000 image compression system, shown in Fig. 1, contains both the wavelet kernels BWFB and the embedded block coding with optimal truncation (EBCOT) coding algorithm. This paper mainly focuses on the optimization design of new BWFB for the JPEG 2000 and does not change the EBCOT coding algorithm.

2.2 PR Conditions of the BWFB

The two channel BWFB for image analysis and synthesis is shown in Fig. 2. The analysis stage contains two filters, a low-pass filter $\widetilde{h}$ and a high-pass filter $\widetilde{g}$, both followed by downsampling for the forward transform. From this BWFB the image can be constructed in the synthesis stage using the inverse transform by first performing an upsampling step and then using two synthesis filters, a low-pass filter h and a high-pass filter g. These synthesis filters are needed for smoothing because the upsampling step is done by inserting a zero in between every two samples.

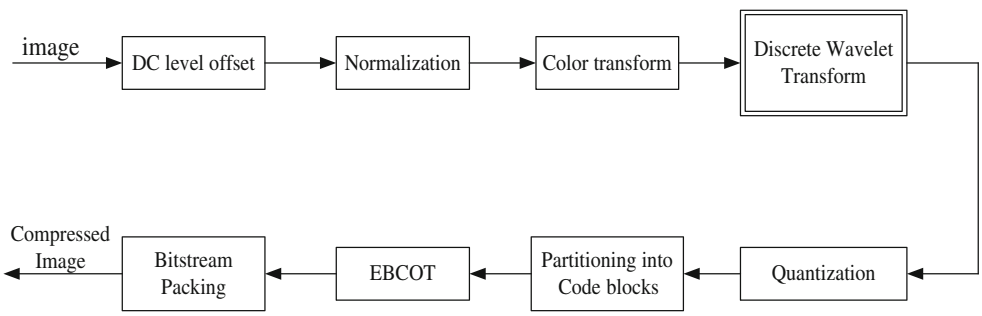

Figure 1 Block diagram of the JPEG2000 image compression system.

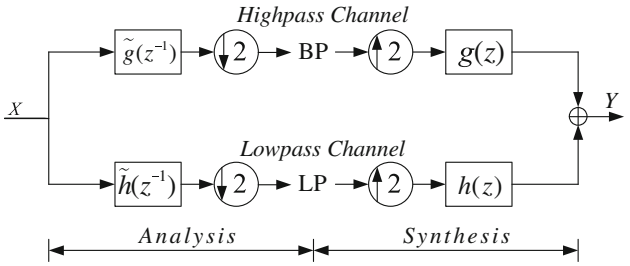

Figure 2 Two channel filter banks for image analysis and synthesis.

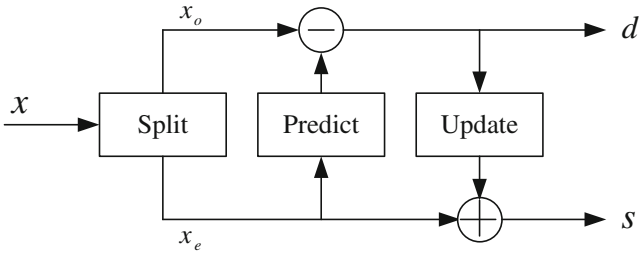

Figure. 3 Filtering structure of Lifting scheme implementation.

In Fig. 2, the PR conditions of the BWFB for image compression are given by

$$\begin{cases} h(z)\widetilde{h}(z^{-1}) + g(z)\widetilde{g}(z^{-1}) = 2 \\ h(z)\widetilde{h}(-z^{-1}) + g(z)\widetilde{g}(-z^{-1}) = 0 \end{cases} \tag{1}$$

If the PR conditions are satisfied, all the aliasing caused by the subsampling will be canceled during the image reconstruction. The first formula shows a pure delay namely no-distortion and the second shows no-aliasing in the JPEG 2000 image transform based on the above BWFB.

2.3 The Lifting Scheme Implementation for the DWT

The wavelet lifting scheme has been introduced for efficient computation of the DWT in the BWFB, and is recommended by the JPEG 2000 standard for implementing the DWT. Its main advantage with respect to the classical DWT structure lies in its improved computational efficiency, and in enabling a new method for the BWFB design. The lifting scheme implementation of the DWT is shown in Fig. 3.

In Fig. 2, the polyphase representation of the BWFB $\{h(z), g(z), \widetilde{h}(z), \widetilde{g}(z)\}$ are as follows

$$\begin{cases} h(z) = h_e(z^2) + z^{-1}h_o(z^2) \\ g(z) = g_e(z^2) + z^{-1}g_o(z^2) \\ \widetilde{h}(z) = \widetilde{h}_e(z^2) + z^{-1}\widetilde{h}_o(z^2) \\ \widetilde{g}(z) = \widetilde{g}_e(z^2) + z^{-1}\widetilde{g}_o(z^2) \end{cases} \tag{2}$$

and $h_e(z)$ and $h_o(z)$, $g_e(z)$ and $g_o(z)$, representing the even and odd coefficients items respectively, are given as follows

$$\begin{cases} h_e(z) = \sum_k h_{2k} z^{-k} \\ h_o(z) = \sum_k h_{2k+1} z^{-k} \\ g_e(z) = \sum_k g_{2k} z^{-k} \\ g_o(z) = \sum_k g_{2k+1} z^{-k} \end{cases} \tag{3}$$

Application of Fig. 3 to Fig. 2 results in Fig. 4, where $\widetilde{P}(z)$, a polyphase matrix, later on used to build a flexible DWT based on a lifting scheme, is given by

$$\widetilde{P}(z) = \begin{bmatrix} \widetilde{h}_e(z) & \widetilde{h}_o(z) \\ \widetilde{g}_e(z) & \widetilde{g}_0(z) \end{bmatrix} \tag{4}$$

Additionally, polyphase matrix $P(z)$, the dual of $\widetilde{P}(z)$, is used for the inverse DWT and given by the following equation

$$P(z) = \begin{bmatrix} h_e(z) & g_e(z) \\ h_o(z) & g_o(z) \end{bmatrix} \tag{5}$$

From Fig. 4 it follows that the PR condition for the BWFB can now be written as

$$P(z)\widetilde{P}(z^{-1})^T = I \tag{6}$$

If the polyphase matrix $P(z)$ has determinant 1, filter pair (h, g) is complementary, and from Eq. 6 it follows that filter pair $(\widetilde{h}, \widetilde{g})$ is also complementary. Moreover, here not only will $P(z)$ be invertible but we also can obtain

$$\begin{cases} \widetilde{h}_e(z) = g_o(z^{-1}) \\ \widetilde{h}_o(z) = -g_e(z^{-1}) \\ \widetilde{g}_e(z) = -h_o(z^{-1}) \\ \widetilde{g}_o(z) = h_e(z^{-1}) \end{cases} \tag{7}$$

Therefore, the DWT implementation based on a lifting scheme only requires the calculation of a filter pair (h, g) in the BWFB for image compression applications. Note that $h_e(z)$ and $h_o(z)$ have to be relatively prime because any common factor would also divide the determinant of $P(z)$, which we know to be equal to 1. We can thus run the Euclidean algorithm starting from $h_e(z)$ and $h_o(z)$, and the greatest common divisor (GCD) will be monomial. Given the non-uniqueness of the division we can always choose the quotients $q_i(z)$ such

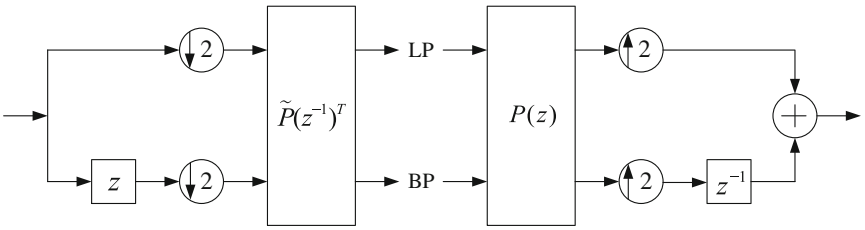

Figure 4 Two channel BWFB for image analysis and synthesis using polyphase matrices.

that the GCD is a constant. Let this non-zero constant be K. We thus have that

$$\begin{bmatrix} h_e(z) \\ h_o(z) \end{bmatrix} = \prod_{k=1}^{n} \begin{bmatrix} q_k(z) & 1 \\ 1 & 0 \end{bmatrix} \begin{bmatrix} K \\ 0 \end{bmatrix} \tag{8}$$

where n is a number of iterate step of Euclidean algorithm using $h_e(z)$ and $h_o(z)$. Similarly, the following formula can be obtained

$$\begin{bmatrix} g_e(z) \\ g_o(z) \end{bmatrix} = \prod_{k=1}^{m} \begin{bmatrix} q_k(z) & 1 \\ 1 & 0 \end{bmatrix} \begin{bmatrix} K \\ 0 \end{bmatrix} \tag{9}$$

where m is a number of iterate step of Euclidean algorithm using $g_e(z)$ and $g_o(z)$.

Then the polyphase matrix $P(z)$ in the synthesis stage can be expressed by

$$P(z) = \begin{bmatrix} h_e(z) & g_e(z) \\ h_o(z) & g_o(z) \end{bmatrix} = \begin{bmatrix} K & 0 \\ 0 & 1/K \end{bmatrix} \prod_{i=1}^{n} \begin{bmatrix} 1 & s_i(z) \\ 0 & 1 \end{bmatrix} \begin{bmatrix} 1 & 0 \\ t_i(z) & 1 \end{bmatrix} \tag{10}$$

where $s_i(z)$and $t_i(z)$ represents lifting and dual lifting. Similarly, the polyphase matrix $\widetilde{P}(z)$ in the analysis stage can be given by

$$\widetilde{P}(z) = \begin{bmatrix} 1/K & 0 \\ 0 & K \end{bmatrix} \prod_{i=1}^{n} \begin{bmatrix} 1 & 0 \\ -s_i(z^{-1}) & 1 \end{bmatrix} \begin{bmatrix} 1 & -t_i(z^{-1}) \\ 0 & 1 \end{bmatrix} \tag{11}$$

We know that the z-transform of a FIR filter is given by

$$f(z) = \sum_{k=m}^{n} f_k z^{-k} \tag{12}$$

This summation is also known as a Laurent polynomial. A Laurent polynomial differs from a normal polynomial in that it can have negative exponents. The degree of a Laurent polynomial f is defined as $|f| = n - m$. Note that in case $|h_o(z)| > |h_e(z)|$, the first quotient $q_1(z)$ equals zero. Here, we can always assume that n is even. Indeed if n is odd, we can multiply the $h(z)$ filter with z and $g(z)$ with $-z^{-1}$. This does not change the determinant of the polyphase matrix. To design the wavelet kernels BWFB for the JPEG2000 standard part-2, we assume that a BWFB family as shown in Fig. 2 and the four filters are expressed as follows:

$$\begin{cases} h(z) = h_0 + \sum_{k=1}^{n} h_k (z^k + z^{-k}) \\ g(z) = g_0 + \sum_{k=1}^{m} g_k (z^k + z^{-k}) \end{cases} \tag{13}$$

$$\begin{cases} \widetilde{h}(z) = -z^{-1} g(-z^{-1}) \\ \widetilde{g}(z) = z^{-1} h(-z^{-1}) \end{cases} \tag{14}$$

where $|h(z)| > |g(z)|$, and the coefficients of $h(z)$ and $g(z)$ are denoted by $h_k, k = 1, 2, \cdots, n$ and $g_k, k = 1, 2, \cdots, m$, respectively. So that the total numbers of coefficients of both the filter $h(z)$ and $g(z)$ equals $2n$+1, $2m$+1, respectively. From wavelet properties and its normalization condition we can get

$$\begin{cases} h_0 + 2\sum_{k=1}^{n} h_k = 1 \\ g_0 + 2\sum_{k=1}^{m} g_k = 1 \end{cases} \tag{15}$$

Moreover, the Eq. 13 resulting in the following truths based on the wavelet properties,

$$\left. \frac{d^k h(z)}{dz^k} \right|_{z=-1} = 0, \quad k = 0, 1, 2, \cdots, n-1 \tag{16}$$

According to Eqs. 2 and 13 we can represent the even and odd coefficients items respectively, as follows

$$\begin{cases} h_e(z) = h_0 + h_2(z + z^{-1}) + \cdots + h_n(z^{n/2} + z^{-n/2}) \\ h_o(z) = h_1(z+1) + h_3(z^2 + z^{-1}) + \cdots + h_{n-1}(z^{n/2} + z^{-(n-2)/2}) \end{cases} \tag{17}$$

$$\begin{cases} g_e(z) = g_0 + g_2(z + z^{-1}) + \cdots + h_m(z^{m/2} + z^{-m/2}) \\ g_o(z) = g_1(z+1) + g_3(z^2 + z^{-1}) + \cdots + g_{m-1}(z^{m/2} + z^{-(m-2)/2}) \end{cases} \tag{18}$$

The polyphase matrix $P(z)$ can be factored into a product of triangular matrices with polynomials in $(1+z)$ or $(1+z^{-1})$, by using the Euclidean algorithm resulting in the following equation

$$P(z)=\begin{bmatrix} h_e(z) & g_e(z) \\ h_o(z) & g_o(z) \end{bmatrix}=\begin{bmatrix} K & 0 \\ 0 & 1/K \end{bmatrix}\prod_{i=1}^{n/2}\begin{bmatrix} 1 & \alpha_{2i-1}(1+z^{-1}) \\ 0 & 1 \end{bmatrix}\begin{bmatrix} 1 & 0 \\ \alpha_{2i}(1+z) & 1 \end{bmatrix} \tag{19}$$

where α_{2i-1} and α_{2i} also are lifting and dual lifting steps in the lifting scheme. The factors $(1+z^{-1})$ and $(1+z)$ are alternant with real coefficients; the former is lifted during low-pass filtering, the latter is lifted during high-pass filtering, and the first step is a low-pass lifting step. Note that the algorithm finishes for the number of lifting steps in the filter $h(z)$ is bounded by $|h_o(z)|+1=n/2-[-(n-2)/2]=n$, and the total number of lifting parameters is $n+1$ including scaling factor K. Since the total numbers of coefficients of the long filter $h(z)$ equals also $n+1$, then according to Eq. 19 all the filter coefficient in both the filter $h(z)$ and $g(z)$ can completely be expressed by using the lifting parameters, as follows

$$\begin{cases} h_k=f_{h_k}(\alpha_1,\alpha_2,\cdots,\alpha_n) \\ g_k=f_{g_k}(\alpha_1,\alpha_2,\cdots,\alpha_m) \end{cases} \tag{20}$$

where f_{h_k} denote a function relationship of lowpass filter $h(z)$ with respect to $\alpha_1,\alpha_2,\cdots,\alpha_n$, f_{g_k} denote a function relationship of highpass filter $g(z)$ with respect to $\alpha_1,\alpha_2,\cdots,\alpha_m$, respectively.

In addition, the Eq. 20 can be substituted into the Eqs. 15 and 16, then resulting in the following equations

$$\begin{cases} f_n(\alpha_1,\alpha_2,\cdots,\alpha_n)=1 \\ f_m(\alpha_1,\alpha_2,\cdots,\alpha_m)=1 \end{cases} \tag{21}$$

$$f_{d_k}(\alpha_1,\alpha_2,\cdots,\alpha_n)=0,\quad k=1,2,\cdots,n-2 \tag{22}$$

where f_n denote a normalization relation for the coefficients of lowpass filter $h(z)$, f_m denote a normalization relation for the coefficients of highpass filter $g(z)$, f_{d_k} denote vanishing moment condition in wavelet theory, respectively. Furthermore, the BWFB have n+1 lowpass and m+1 highpass filter coefficients, 2 normalization condition, $n-2$ vanishing moment from Eqs. 20, 21 and 22, then BWFB give us in total (n+1)+(m+1)+2+(n−2)=2n+m+2 independent equations for these 2n+m+3 variables including n+1 lowpass and m+1 highpass filter coefficients, n lifting parameters and 1 scale factor K. Therefore, the variables can be expressed as function with respect to a single lifting parameter α_i such as α_1, as follows.

$$\alpha_i=f_{\alpha_i}(\alpha_1),\ i\neq 1 \tag{23}$$

According to the Eqs. 20 and 23 we can obtain below

$$\begin{cases} h_k=f^1_{h_k}(\alpha_1) \\ g_k=f^1_{g_k}(\alpha_1) \end{cases} \tag{24}$$

The Eq. 24 denotes a function relationship of lowpass filters $h(z)$ and highpass filter $g(z)$ with respect to α_1, where the superscript on f in Eq. 24 correspond to the subscript of α_1. In fact, the Eq. 23 can also be rewritten below

$$\alpha_i=f^j_{\alpha_i}(\alpha_j),\quad i\neq j \tag{25}$$

Similarly, the superscript on f in Eq. 25 correspond to the subscript of α_j. Based on Eq. 25 we can obtain more truths that all the lifting parameters are expressed only one free variable with exception of all the lifting parameters α_i and scaling factor K such as ξ, as follows

$$\alpha_i=f^{\xi}_{\alpha_i}(\xi) \tag{26}$$

Then the first lifting parameter α_1 is given by using the Eq. 26

$$\alpha_1=f^{\xi}_{\alpha_1}(\xi) \tag{27}$$

Combining the Eqs. 24 and 27 the following equations can be written by

$$\begin{cases} h_k=f^{\xi}_{h_k}(f^{\xi}_{\alpha_1}(\xi)) \\ g_k=f^{\xi}_{g_k}(f^{\xi}_{\alpha_1}(\xi)) \end{cases} \tag{28}$$

In fact, the Eq. 24 can also be rewritten, as follows

$$\begin{cases} h_k = f_{h_k}^{i}(\alpha_i) \\ g_k = f_{g_k}^{i}(\alpha_i) \end{cases} \tag{29}$$

Finally, we can derive all coefficients of the BWFB in the Eq. 13 as one dimensional functions with respect to ξ according to Eqs. 26 and 29, resulting in

$$\begin{cases} h_k = f_{h_k}^{\alpha_i}(f_{\alpha_i}^{\xi}(\xi)) \\ g_k = f_{g_k}^{\alpha_i}(f_{\alpha_i}^{\xi}(\xi)) \end{cases} \tag{30}$$

Therefore, Eq. 30 not only greatly reduces complexity of the optimization design of the BWFB but is also convenient for the analysis with regard to the coding gain, regularity properties, rate distortion in biorthogonal subband coding systems. Particularly Eq. 30 is convenient for estimation of the PSNR of the reconstructed images.

2.4 Regularity Condition of the BWFB

The regularity condition is crucial for the design and optimization of the BWFB. To achieve symmetrical BWFB $\{\widetilde{h}(z), \widetilde{g}(z), h(z), g(z)\}$ for extending the wavelet kernels of the JPEG2000 standard part-2, the regularity condition is required. By using Daubechies' theorem, we can determine the interval with respect to the free variable ξ for designing and optimizing BWFB that satisfy PR condition for implementing the DWT based on a lifting scheme.

3 General Image Modeling

An autoregressive (AR) process is generated by passing the white noise process $W(n)$ of the power spectral density (PSD). The difference equation which generates the AR process [15] is

$$X(n) - \sum_{i=1}^{L} b_i X(n-i) = W(n) \tag{31}$$

where process $X(n)$ is called an AR (N) process or Nth order Markov process, and the b_i are called autoregressive constants. However, the autocorrelation function (ACF) of the output process $X(n)$ can be calculated for any given set of coefficients $b_i, i = 1, 2, \cdots, L$. This can be seen by multiplying $X(n)$ with $x(n-k)$ and taking expectations on both sides of the equation, and by noting that $E[W(n)X(n-k)] = 0, k > 0$ because the signal $W(n)$ is by definition uncorrelated with past outputs. The PSD of a first-order Markov process is given by

$$S_{xx}(e^{j\omega}) = \frac{1}{1 + \rho^2 - 2\rho\cos\omega} \tag{32}$$

Note that the AR constant b_1 is the first normalized ACF value of the AR (1) process, and let $b_1 = \rho = 0.95$.

Therefore, we can take a first-order Markov process as an input image model, and use two-channel filter banks to implement subband coding, in addition, we can calculate the maximum value of the coding gain and corresponding value of free variable ξ.

4 Optimization Design for a BWFB

We adopt two channel filter banks to implement the subband coding with an input image of the model in section 3. The BWFB satisfies the PR condition, therefore it can be achieved to remove the aliasing distortion, the amplitude and phase distortion for the reconstructed image. In this section, we will design the BWFB based on the Vaidyanathan optimal coding gain criterion [16]. In Fig. 2, the variance of the subband signal $x_k(n), k = 0, 1$ can be obtained as follows

$$\sigma_{x_k}^2 = \frac{1}{2\pi}\int_{-\pi}^{+\pi} S_{xx}(e^{j\omega})\left|H_k(e^{j\omega})\right|^2 d\omega \tag{33}$$

The input random first-order Markov process with Gaussian white noise can be calculated by using Eq. 32. $H_k(z), k = 0, 1$ denote $\widetilde{h}(z)$ and $\widetilde{g}(z)$ the lowpass filter and highpass filter of the analysis stage defined in section 2, respectively. The subband noises are uncorrelated and they remain uncorrelated after passing through the synthesis filter. Then the output noise variance on the subband coding system can be written as

$$\sigma_{SBC}^2 = \frac{C}{W}\sum_{k=0}^{W-1} 2^{-2b_k}\frac{1}{2\pi}\int_{-\pi}^{+\pi}\left|G_k(e^{j\omega})\right|^2 d\omega \cdot \frac{1}{2\pi}\int_{-\pi}^{+\pi} S_{xx}(e^{j\omega})\left|H_k(e^{j\omega})\right|^2 d\omega \tag{34}$$

where, W=2, C is a constant that depends on the statistics of $x_k(n)$, b_k, k=0, 1 are the numbers of bits allocated to the two channel filter banks, and $G_k(z)$, k=0, 1 corresponds to lowpass filter $h(z)$ and highpass filter $g(z)$ of the synthesis stage defined in section 2, respectively. If we quantize the input signal to these numbers of bits,

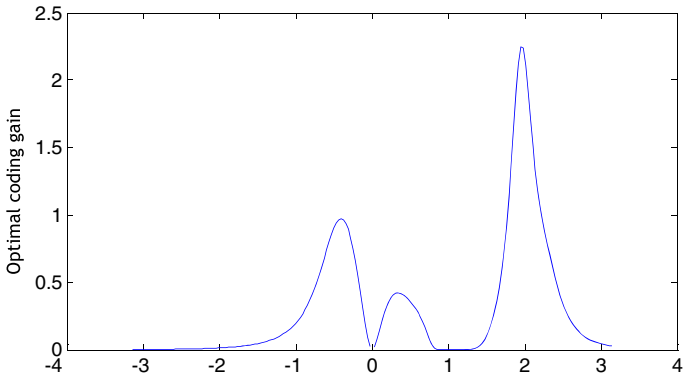

Figure 5 Free variable ξ of the new 9/7 BWFB.

Table 1 Coding performances using 9/7 BWFB defined by different variable ξ (PSNR/dB), and within parentheses indicates a variable ξ.

Bit rate=0.25 bpp					
43.192582(1.00)	44.680161(1.01)	48.446302(1.02)	48.464296(1.03)	48.856082(1.04)	48.554753(1.05)
48.732624(1.06)	48.909152(1.07)	48.830711(1.08)	48.807920(1.09)	48.707917(1.10)	48.767470(1.11)
48.667138(1.12)	48.587628(1.13)	48.484155(1.14)	48.501623(1.15)	48.464763(1.16)	48.308489(1.17)
48.298717(1.18)	48.240907(1.19)	48.085813(1.20)	48.060494(1.21)	47.901344(1.22)	47.865897(1.23)
47.700875(1.24)	47.576375(1.25)	47.304045(1.26)	47.165760(1.27)	47.080027(1.28)	46.793639(1.29)
46.551740(1.30)					
Bit rate=0.125 bpp					
36.551740(1.00)	37.109991(1.01)	42.524363(1.02)	44.222247(1.03)	46.473645(1.04)	45.911562(1.05)
46.347605(1.06)	46.728545(1.07)	46.701913(1.08)	46.797134(1.09)	46.782938(1.10)	47.001525(1.11)
46.994139(1.12)	46.976332(1.13)	46.910748(1.14)	47.058549(1.15)	47.022296(1.16)	47.172372(1.17)
47.147738(1.18)	47.131913(1.19)	47.031164(1.20)	47.031560(1.21)	46.951704(1.22)	46.935263(1.23)
46.856938(1.24)	46.774074(1.25)	46.574580(1.26)	46.474423(1.27)	46.384795(1.28)	46.194295(1.29)
45.911656(1.30)					
Bit rate=0.0625 bpp					
25.911656(1.00)	30.044943(1.01)	38.850235(1.02)	40.338173(1.03)	42.255825(1.04)	41.893182(1.05)
42.154643(1.06)	42.383937(1.07)	42.450394(1.08)	42.444969(1.09)	42.566689(1.10)	42.860920(1.11)
42.856777(1.18)	42.895691(1.19)	42.783006(1.20)	42.991442(1.21)	42.895361(1.22)	42.882458(1.23)
43.110399(1.24)	43.109892(1.25)	43.146573(1.26)	43.147197(1.27)	43.062226(1.28)	43.064832(1.29)
43.027509(1.12)	42.926852(1.13)	42.841604(1.14)	42.666601(1.15)	42.516612(1.16)	42.536721(1.17)
42.376745(1.30)					
Bit rate=0.03125 bpp					
22.376745(1.00)	23.278374(1.01)	36.029273(1.02)	37.105421(1.03)	37.950865(1.04)	37.610988(1.05)
38.377173(1.06)	38.708739(1.07)	38.634700(1.08)	38.611069(1.09)	38.593074(1.10)	38.887561(1.11)
38.835048(1.18)	38.866044(1.19)	38.940916(1.20)	38.984357(1.21)	38.815214(1.22)	38.937806(1.23)
38.842494(1.24)	39.114535(1.25)	38.975289(1.26)	39.225545(1.27)	39.273580(1.28)	39.193119(1.29)
39.170421(1.12)	39.120877(1.13)	38.910224(1.14)	38.800341(1.15)	38.679747(1.16)	38.409165(1.17)
38.362917(1.30)					
Bit rate=0.015625 bpp					
18.362917(1.00)	20.843106(1.01)	31.854331(1.02)	32.458420(1.03)	32.743809(1.04)	33.027853(1.05)
33.445628(1.06)	33.425510(1.07)	33.733438(1.08)	33.784569(1.09)	33.894714(1.10)	33.910355(1.11)
33.898625(1.18)	34.172572(1.19)	34.194232(1.20)	34.200707(1.21)	34.068329(1.22)	34.266891(1.23)
34.188305(1.24)	34.279474(1.25)	34.491754(1.26)	34.233165(1.27)	34.407422(1.28)	34.483333(1.29)
34.341064(1.12)	34.342284(1.13)	34.540114(1.14)	34.162129(1.15)	34.003458(1.16)	33.816891(1.17)
33.502779(1.30)					

Table 2 All coefficients of new 9/7 BWFB.

number	analysis filter		synthesis filter	
k	low-pass filter $\widetilde{h}$	high-pass filter $\widetilde{g}$	low-pass filter h	high-pass filter g
0	43/80	5897/4600	5897/4600	43/80
±1	93/320	2393/4600	2393/4600	93/320
±2	−3/160	−17/92	−17/92	−3/160
±3	−13/320	561/18400	561/18400	−13/320
±4		403/9200	403/9200	

without any subband decomposition, i.e., just pulse coding modulation (PCM), the noise variance would be

$$\sigma_{PCM}^2 = C2^{-2b}\sigma_x^2 = C2^{-2b}\frac{1}{2\pi}\int_{-\pi}^{+\pi} S_{xx}(e^{j\omega})d\omega \tag{35}$$

where b is the average bit rate. Therefore we can obtain the coding gain which is defined as the ratio of the above variances as follows

$$G = \frac{\sigma_{PCM}^2}{\sigma_{SBC}^2} = \left[2^{-2b}\frac{1}{2\pi}\int_{-\pi}^{+\pi} S_{xx}(e^{j\omega})d\omega\right] \div \left[\frac{1}{W}\sum_{k=0}^{W-1} 2^{-2b_k}\frac{1}{2\pi}\int_{-\pi}^{+\pi}\left|G_k(e^{j\omega})\right|^2 d\omega \cdot \frac{1}{2\pi}\int_{-\pi}^{+\pi} S_{xx}(e^{j\omega})\left|H_k(e^{j\omega})\right|^2 d\omega\right] \tag{36}$$

One of the optimization steps is an optimal bit allocation. We can make this step now and minimize the denominator. The optimal bit allocation turns the sum in the denominator into a product. So we can obtain the following expression for the coding gain under optimal bit allocation

$$G_{opt}(\xi) = \left[\frac{1}{2\pi}\int_{-\pi}^{+\pi} S_{xx}(e^{j\omega})d\omega\right] \div \left[\left[\prod_{k=0}^{W-1}\frac{1}{2\pi}\int_{-\pi}^{+\pi}\left|G_k(e^{j\omega})\right|^2 d\omega \cdot \frac{1}{2\pi}\int_{-\pi}^{+\pi} S_{xx}(e^{j\omega})\left|H_k(e^{j\omega})\right|^2 d\omega\right]^{1/W}\right] \tag{37}$$

In general, horizontal and vertical relations between adjacent samples of the image are the same, i.e., $\rho_h = \rho_v = \rho = 0.95$. We combine Eqs. 13, 14, 30, 32 and 37 to derive the one dimensional function $G_{opt}(\xi)$ which is optimal subband coding gain with respect to a free variable ξ. Finally, we can obtain the optimal the BWFB which is determined by the maximum coding gain $G_{max}(\xi)$ according to $dG_{opt}(\xi)/d\xi = 0$, thus all the coefficients and the lifting parameters of the BWFB which satisfy the coding gain criterion are determined by Eq. 30.

5 Results and Analysis

5.1 Theoretical Design of the New 9/7 BWFB

In this section, we will present the new 9/7 BWFB with rational coefficients suitable for infrared thermal images using the above design approach in the JPEG2000 framework. The new 9/7 BWFB can also be used as an extension for the JPEG2000 wavelet kernels. From Eq. 13 with n=4 and m=3, we obtain the following lowpass filter $h(z)$ and highpass filter $g(z)$ for the synthesis stage of a new 9/7 BWFB

$$\begin{cases} h(z) = h_0 + \sum_{k=1}^{4} h_k(z^k + z^{-k}) \\ g(z) = g_0 + \sum_{k=1}^{3} g_k(z^k + z^{-k}) \end{cases} \tag{38}$$

Table 3 Lifting parameters of new 9/7 BWFB.

Lifting parameter	parameter values
α_1	−13/6
α_2	−9/400
α_3	100/69
α_4	713/2000
K	40/23

According to Eq. 2, the polyphase representation for the filters $h(z)$ and $g(z)$ on synthesis stage in the new 9/7 BWFB can then be written as

$$\begin{cases} h_e(z) = h_0 + h_2(z + z^{-1}) + h_4(z^2 + z^{-2}) \\ h_o(z) = h_1(z + 1) + h_3(z^2 + z^{-1}) \end{cases} \tag{39}$$

$$\begin{cases} g_e(z) = g_0 + g_2(z + z^{-1}) \\ g_o(z) = g_1(z + 1) + g_3(z^2 + z^{-1}) \end{cases} \tag{40}$$

According to Eq. 19, we can assemble the polyphase matrix of the new 9/7 WBFB as

$$P(z) = \begin{bmatrix} h_e(z) & g_e(z) \\ h_o(z) & g_o(z) \end{bmatrix} = \begin{bmatrix} 1 & \alpha_1(1 + z^{-1}) \\ 0 & 1 \end{bmatrix} \begin{bmatrix} 1 & 0 \\ \alpha_2(1 + z) & 1 \end{bmatrix} \begin{bmatrix} 1 & \alpha_3(1 + z^{-1}) \\ 0 & 1 \end{bmatrix} \begin{bmatrix} 1 & 0 \\ \alpha_4(1 + z) & 1 \end{bmatrix} \begin{bmatrix} K & 0 \\ 0 & 1/K \end{bmatrix} \tag{41}$$

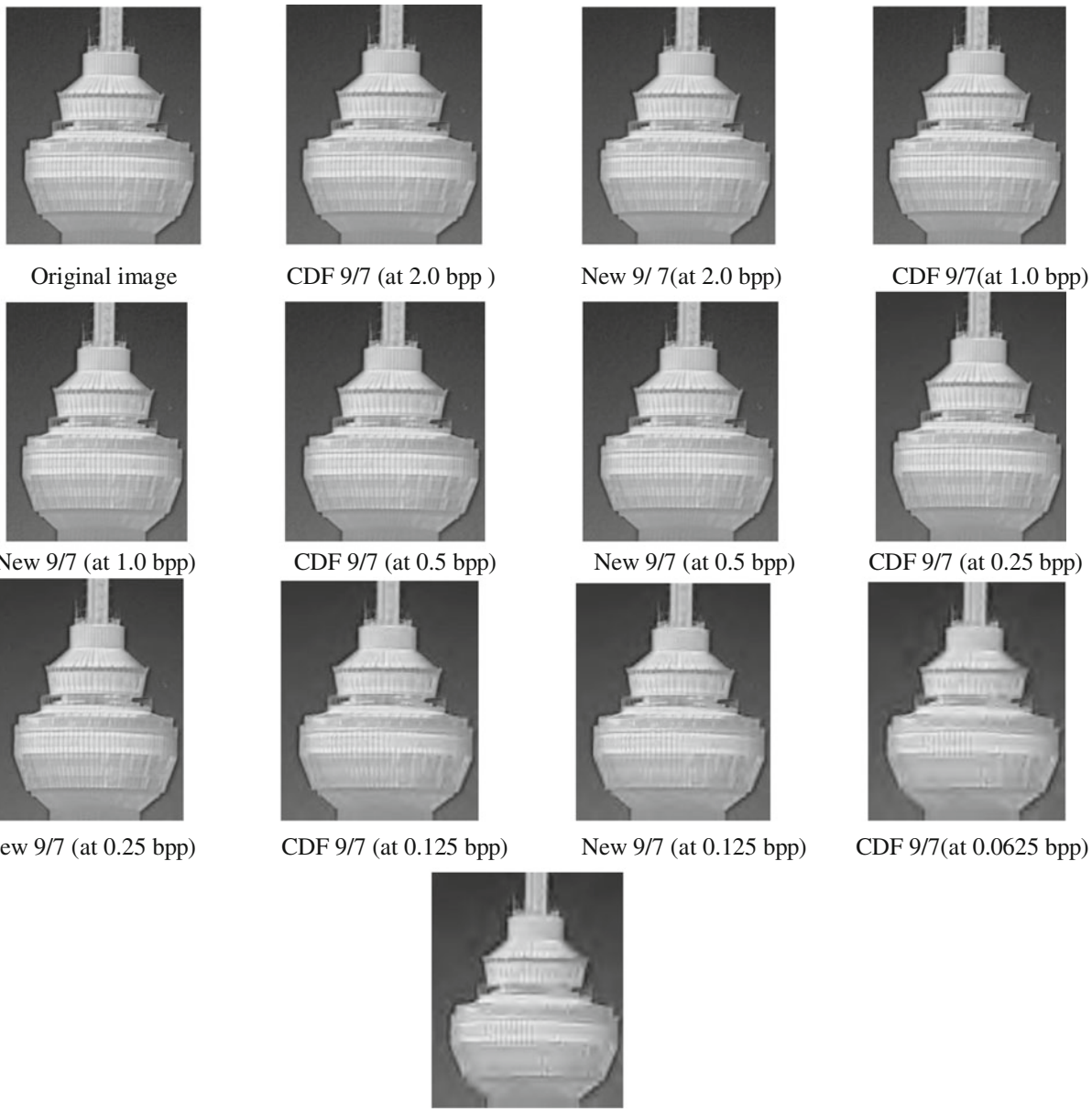

Figure 6 The subjective comparison using new 9/7 BWFB and CDF 9/7 BWFB with Infrared image TelevisionTower.

Substitute Eqs. 39 and 40 into Eq. 41 we thus can obtain

$$P(z)=\begin{bmatrix} h_e(z) & h_o(z) \\ -g_o(z^{-1}) & g_e(z^{-1}) \end{bmatrix}=\begin{bmatrix} h_0+h_2(z+z^{-1})+h_4(z^2+z^{-2}) & h_1(z+1)+h_3(z^2+z^{-1}) \\ -g_1(1+z^{-1})-g_3(z+z^{-2}) & g_0+g_2(z+z^{-1}) \end{bmatrix}= \tag{42}$$

$$\begin{bmatrix} [(1+2\alpha_1\alpha_2+2\alpha_1\alpha_4+2\alpha_3\alpha_4+6\alpha_1\alpha_2\alpha_3\alpha_4) & \\ +(\alpha_1\alpha_2+\alpha_1\alpha_4+\alpha_3\alpha_4+4\alpha_1\alpha_2\alpha_3\alpha_4)(z+z^{-1}) & [(\alpha_2+\alpha_4+3\alpha_2\alpha_3\alpha_4)(z+1)+\alpha_2\alpha_3\alpha_4(z^2+z^{-1})]K \\ +\alpha_1\alpha_2\alpha_3\alpha_4(z^2+z^{-2})]K & \\ [(\alpha_1+\alpha_3+3\alpha_1\alpha_2\alpha_3)(1+z^{-1})+\alpha_1\alpha_2\alpha_3(z+z^{-2})]/K & [(1+2\alpha_2\alpha_3)+\alpha_2\alpha_3(z+z^{-1})]/K \end{bmatrix}$$

The 2×2 matrix in Eq. 42 gives us 4 polynomial equations, in each of which the coefficients of the corresponding powers of z are the same, so the functional relation between coefficients of the new 9/7 BWFB and their corresponding lifting parameters are given below

$$\begin{cases} h_0=(1+2\alpha_1\alpha_2+2\alpha_1\alpha_4+2\alpha_3\alpha_4+6\alpha_1\alpha_2\alpha_3\alpha_4)K \\ h_1=(3\alpha_2\alpha_3\alpha_4+\alpha_2+\alpha_4)K \\ h_2=(\alpha_1\alpha_2+\alpha_1\alpha_4+\alpha_3\alpha_4+4\alpha_1\alpha_2\alpha_3\alpha_4)K \\ h_3=\alpha_2\alpha_3\alpha_4K \\ h_4=\alpha_1\alpha_2\alpha_3\alpha_4K \\ g_0=(2\alpha_2\alpha_3+1)/K \\ g_1=-(3\alpha_1\alpha_2\alpha_3+\alpha_1+\alpha_3)/K \\ g_2=\alpha_2\alpha_3/K \\ g_3=-\alpha_1\alpha_2\alpha_3/K \end{cases} \tag{43}$$

From Eqs. 15 and 16 we can obtain the following equations

$$\begin{cases} h_0+2\sum_{k=1}^{4}h_k=1 \\ g_0+2\sum_{k=1}^{3}g_k=1 \\ h_0+2\sum_{k=1}^{4}(-1)^k h_k=0 \\ g_0+2\sum_{k=1}^{3}(-1)^k g_k=0 \end{cases} \tag{44}$$

Furthermore, substitute Eqs. 43 into Eqs. 44, all the lifting parameters in the new 9/7 BWFB can then be

(a) (b) (c)

(d) (e)

Figure 7 Infrared test images, **a** Building, **b** Pagoda, **c** Bridge, **d** Antenna, **e** Airplane.

expressed as a one dimensional function for a free variable α_1, as follows

$$\begin{cases} \alpha_2 = \frac{1}{4(1+2\alpha_1)^2} \\ \alpha_3 = \frac{-1-4\alpha_1-4\alpha_1^2}{1+4\alpha_1} \\ \alpha_4 = \frac{1}{16}\left[4 - \frac{2+4\alpha_1}{(1+2\alpha_1)^4} + \frac{1-8\alpha_1}{(1+2\alpha_1)^2}\right] \\ K = \frac{2(1+2\alpha_1)}{1+4\alpha_1} \end{cases} . \tag{45}$$

Substitute Eq. 45 into Eq. 43 we then can obtain a one dimensional functions of α_1, as follows

$$\begin{cases} h_0 = \frac{184\alpha_1^3+266\alpha_1^2+125\alpha_1+20}{16(1+2\alpha_1)^2(1+4\alpha_1)} \\ h_1 = \frac{128\alpha_1^3+152\alpha_1^2+58\alpha_1+5}{32(1+2\alpha_1)^2(1+4\alpha_1)} \\ h_2 = -\frac{3+4\alpha_1}{8(1+4\alpha_1)} \\ h_3 = \frac{8\alpha_1^2+6\alpha_1+3}{32(1+2\alpha_1)^2(1+4\alpha_1)} \\ h_4 = \frac{\alpha_1(8\alpha_1^2+6\alpha_1+3)}{32(1+2\alpha_1)^2(1+4\alpha_1)} \\ g_0 = \frac{8\alpha_1+3}{8(1+2\alpha_1)} \\ g_1 = \frac{9\alpha_1+4}{16(1+2\alpha_1)} \\ g_2 = \frac{1}{16(1+2\alpha_1)} \\ g_3 = -\frac{\alpha_1^2}{16(1+2\alpha_1)} \end{cases} . \tag{46}$$

Finally, we can simplify the Eq. 46 using the function relationship $\alpha_1 = \frac{2\xi-1}{4(1-\xi)}$, then resulting in the following equations

$$\begin{cases} h_0 = -(8\xi^3 - 18\xi^2 + 7\xi - 20)/(16\xi) \\ h_1 = (4\xi^3 - 11\xi^2 + 15\xi - 4)/(8\xi) \\ h_2 = (\xi - 2)/(4\xi) \\ h_3 = (4\xi^2 - 7\xi + 4)(\xi - 1)/(8\xi) \\ h_4 = (4\xi^2 - 7\xi + 4)(2\xi - 1)/(32\xi) \\ g_0 = (\xi + 1)/4 \\ g_1 = (2\xi + 7)/32 \\ g_2 = -(\xi - 1)/8 \\ g_3 = -(2\xi - 1)/32 \end{cases} . \tag{47}$$

Moreover, the Eq. 45 can be expressed as one dimensional functions of ξ, as follows

$$\begin{cases} \alpha_1 = \frac{1-2\xi}{4(\xi-1)} \\ \alpha_2 = -(\xi-1)^2 \\ \alpha_3 = \frac{1}{4\xi(\xi-1)} \\ \alpha_4 = \xi^3 - \frac{7\xi^2}{4} + \xi \\ K = 2/\xi \end{cases} . \tag{48}$$

Therefore, we can combine Eqs. 14, 32, 37, 38 and 47 to calculate the $G_{opt}(\xi)$ with respect to the free variable ξ; $G_{opt}(\xi)$ is plotted in Fig. 5, and we can obtain that when ξ=1.9478, the maximum value of $G_{opt}(\xi)$ equals 2.2374 in Fig. 5, such that we can obtain the theoretically optimal 9/7 BWFB by computing Eqs. 47 and 48.

5.2 Optimization Design of the New 9/7 BWFB

Although the 9/7 BWFB designed in section 5.1 is optimal in terms of the Vaidyanathan optimal coding gain criterion, it cannot be applied to the JPEG2000 standard part-2 immediately for image compression applications, because the actual image differs from the image model in section 3. Therefore, we also need to further optimize the above 9/7 BWFB for the actual image and we do so based on the PSNR criterion. Finally, we can obtain the optimal BWFB by determination of the free variable ξ corresponding to maximum PSNR value for a class of images in the extensible JPEG2000 image compression systems [17]. Based on section 2.4, we can see that free variable $\xi \in [0.78, 1.85]$. Finally, we also consider the result in section 5.1, and select the variable interval as $\xi \in [1.00, 1.30]$. In this paper, we establish an image compression verification system, which is based on

Table 4 Comparison of image compression performances between the new 9/7 and CDF 9/7 BWFB (PSNR/dB).

Bit rate(bpp)	BWFB	TelevisionTower	Building	Pagoda	Bridge	Antenna	Airplane
2.0	New 9/7	48.501623	48.402436	48.380536	48.315316	48.172654	47.502043
2.0	CDF 9/7	48.309717	48.283014	48.199168	48.16754	48.056815	47.456554
1.0	New 9/7	47.058549	44.929832	46.162533	45.102093	43.342957	41.920155
1.0	CDF 9/7	47.191826	44.839302	46.121347	45.048428	43.399923	42.056013
0.5	New 9/7	42.991442	38.870313	41.851242	39.473175	38.687127	37.423809
0.5	CDF 9/7	43.029705	39.092671	41.730600	39.610948	38.732974	37.696641
0.25	New 9/7	38.984357	33.504103	37.662346	34.197749	34.968250	34.082748
0.25	CDF 9/7	39.168405	33.567664	37.764544	34.275736	35.098284	34.195657
0.125	New 9/7	34.200707	28.903056	33.715839	30.159875	31.378639	30.845426
0.125	CDF 9/7	34.284778	28.837952	33.482506	30.011322	31.409393	30.969722
0.0625	New 9/7	30.340684	24.967672	29.893755	27.044121	28.087401	27.602140
0.0625	CDF 9/7	30.276590	25.095483	29.838113	26.992470	27.825338	27.929777

Table 5 The complexity of lifting implementation using the CDF 9/7 BWFB.

Lifting parameters	binary representation (64 bit double precision floating method)	multipliers
−1.586134342	1011 1111 1111 1001 0110 0000 1100 1110 0110 0111 0101 1111 0011 1101 0101 1011	41
−0.052980118	1011 1111 1010 1011 0010 0000 0011 0101 1100 1000 1110 1111 0101 1100 1001 0111	36
0.882911075	0011 1111 1110 1100 0100 0000 1100 1110 1001 0101 1110 0000 0011 0011 1010 1010	32
0.443506852	0011 1111 1101 1100 0110 0010 0110 1010 1001 0000 0111 0000 0000 1110 1101 0111	32
1.149604398	0011 1111 1111 0010 0110 0100 1100 0111 1001 0100 1100 1011 1111 0110 1101 1011	37

reference software Jasper 1.701.0 with an EBCOT coding algorithm in the JPEG2000 standard part-2. It supports multi-kernels BWFB for the image compression applications, and all the BWFB coefficients and their lifting parameters only depend on the free lifting parameter ξ. In addition, we select 6 test images from infrared thermal imaging. The test images shows TelevisionTower, Building, Pagoda, Bridge, Antenna, and Airplane, at a resolution of 302×366, 578×386, 545×334, 578×386, 579×389, 579×389 pixels with 8 bit depth. To find the optimal 9/7 BWFB for infrared thermal images, we apply image compression to all the test images and compute the PSNR values for different values of control variable ξ. The results are shown in Table 1 and show that, for $\xi=1.15$, the maximum PSNR value of a reconstructed image in the extensible JPEG2000 image compression system is obtained. Therefore, we can determine all the new 9/7 BWFB coefficients and their lifting parameters with rational coefficients using Eqs. 47 and 48 for optimal 9/7 BWFB as shown in Tables 2 and 3. The new 9/7 BWFB, compared to CDF 9/7 BWFB with irrational coefficients in the JPEG 2000 standard part-1, not only takes less computational complexity but is also more suitable for implementation in VLSI hardware.

Moreover, using the test images in Fig. 7 we compared the new 9/7 BWFB to CDF 9/7 BWFB in JPEG2000 standard part-1 for the image compression performances at different bit rates as shown in Table 4. The experimental results show that the PSNR of the reconstructed image by using new 9/7 BWFB is only 0.030754–0.272832 dB at 1.0, 0.5, 0.25 and 0.125 bpp less than CDF 9/7 BWFB in the JPEG2000 standard part-1, but is higher 0.191906 and 0.262063 dB at 2.0 and 0.0625 bpp, respectively.

In order to illustrate performances of the new 9/7 BWFB, we compared the complexity of the proposed 9/7 BWFB with CDF 9/7. The lifting implementation of CDF 9/7 with irrational coefficients in the JPEG2000 standard part-1 needs to do 178 multiplication, however, we proposed 9/7 BWFB with rational coefficients needs only to do 39 multiplication. The complexity of VLSI hardware implementation between new 9/7 and CDF 9/7 BWFB shown in Tables 5 and 6.

Furthermore, the subjective comparison results are good for infrared thermal images at bit rate 2.0, 1.0, 0.5, 0.25, 0.125 and 0.0625 bpp as shown in Fig. 6, and also as good as CDF 9/7 BWFB in the JPEG2000 standard part-1.

6 Conclusions

In this paper we propose a procedure to carry out a fast and efficient design of the BWFB for the JPEG2000 standard part-2. At the same time, we exploit 9/7 BWFB for a design example to find an optimal 9/7 BWFB with rational coefficients for infrared thermal images. The new 9/7 BWFB with rational coefficients and lifting parameters can be obtained for the JPEG2000 standard part-2. The computational complexity of the new 9/7 BWFB with rational coefficients is greatly reduced compared to the CDF 9/7 BWFB with irrational coefficients in the JPEG2000 standard part-1. Furthermore, the new 9/7 BWFB outperforms CDF 9/7 BWFB of JPEG2000 standard part-1 in computation time, memory cost, and implementation complexity in VLSI hardware. Therefore, the new 9/7 BWFB are more suitable for real-time image transmission in a network and hardware implementation for object detection, target tracking and monitoring. The approach presented in this paper cannot only be used to design the optimal 9/7 BWFB with rational coefficients but also to design a BWFB with other length in the JPEG2000 framework.

Table 6 The complexity of lifting implementation using the new 9/7 BWFB.

Lifting parameters	binary representation (16 bit fixed point method)	multipliers
−13/6	0010 1010 1010 1011	8
−9/400	0000 0101 1100 0010	5
100/69	0111 0011 0000 0011	7
713/2000	0101 1011 0100 0011	8
40/23	1011 1101 0011 0111	11

Acknowledgment This work was supported by the Chinese national natural science foundation under grants 90920301 and 51075317, and 973 project of national key basic research of China (No. 2007CB311005).

References

1. Antonini, M., Barlaud, M., & Daubechies, I. (1992). Image coding using wavelet transform. *IEEE Transactions on Image Processing, 1*(2), 205–220.
2. JPEG2000 Image Coding System, Part 1 (Core), ISO/IEC Int'l. Standard 15444–1, ITU-T Rec. T.800. Int'l. Org. for Standardization, 2003.
3. JPEG2000 Image Coding System, Part 2 (Extensions), ISO/IEC Int'l. Standard 15444–2, ITU-T Rec. T.800. Int'l. Org. for Standardization, 2004.
4. Sweldens, W. (1996). The lifting scheme: a custom-design construction of biorthogonal wavelets. *Journal Applied and Computational Harmonic Analysis, 3*(2), 186–200.
5. Sweldens, W. (1997). The lifting scheme: a construction of second generation wavelets. *SIAM Journal on Mathematical Analysis, 29* (2), 511–546.
6. Daubechies, I., & Sweldens, W. (1998). Factoring wavelet transforms into lifting steps. *Journal of Fourier Analysis and Applications, 4*(3), 247–269.
7. Cohen, A., Daubechies, I., & Feauveau, J. C. (1992). Biorthogonal bases of compactly supported wavelets. *Journal Communications on Pure Applied Mathematics, 45*(5), 485–560.
8. Ohno, S., & Sakai, H. (1996). Optimization of filter banks using cyclostationary spectral analysis. *IEEE Transactions on Signal Processing, 44*(11), 2718–2725.
9. Vaidyanathan, P. P., & Kirac, A. (1998). Results on optimal biorthogonal filter banks. *IEEE Transactions Circuits and Systems-2: Analog and Digital Signal Processing, 45*(8), 932–947.
10. Tewfik, A. H., Sinha, D., & Jorgensen, P. (1992). On the optimal choice of a wavelet for signal representation. *IEEE Transactions on Information Theory, 38*(2), 747–765.
11. Tay, D. B. H. (2002). Two-stage, least squares design of biorthogonal filter banks. *IEE Proceedings, Vision, Image and Signal Processing, 149*(6), 341–346.
12. Moulin, P., Anitescu, M., et al. (2000). Theory of rate-distortion optimal, constrained filter banks application to IIR and FIR biorthogonal design. *IEEE Transactions on Signal Processing, 48* (4), 1120–1132.
13. Liu, Z. D., Zheng, N. N., Liu, Y. H., & V. d. Wetering, H (2007). Optimization design of biorthogonal wavelets for embedded image coding. *IEICE Transactions on Information and Systems*, *E90-D*(2), 569–578.
14. Guo, S. M., Chang, W. H., Tsai, J. S.-H., Zhuang, B. L., & Chen, L. C. (2008). JPEG 2000 wavelet filter design framework with chaos evolutionary programming. *Elsevier, Signal Processing, 88* (10), 2542–2553.
15. Jayant, N. S., & Noll, P. (1984). *Digital coding of waveforms: principles and applications to speech and video*. Englewood Cliffs: Prentice-Hall.
16. Djokovic, I., & Vaidyanathan, P. P. (1996). On optimal analysis/synthesis filters for coding gain maximization. *IEEE Transactions on Signal Processing, 44*(5), 1276–1279.
17. Yang, G. A., & Zheng, N. N. (2008). A optimization algorithm for biorthogonal wavelet filter banks design. *International Journal of Wavelets, Multiresolution and Information Processing, 6*(1), 51–63.

Guoan Yang received the B.S. degree from Jilin University China, and M.S. degree from Tokyo Metropolitan University Japan in 1986 and 1993, respectively. From 1993-2001, he was a researcher fellow with Hertz co. Ltd in Japan. He returned to Xi'an Jiaotong University in 2001, and received a Ph.D. degree in pattern recognition and intelligent system, Xi'an Jiaotong University, Xi'an, China, in 2007. He is an associate professor at Xi'an Jiaotong University and an IEEE member. His research interests include vision computing, image processing, and wavelet theory and multiscale Geometric analysis etc.

Huub van de Wetering studied Mathematics at the Technische Universiteit Eindhoven, The Netherlands, obtained his Ph.D. degree there, and is now employed as an assistant professor at the Department of Mathematics and Computer science. His research interests are computer graphics, implicit surfaces, and information visualization.

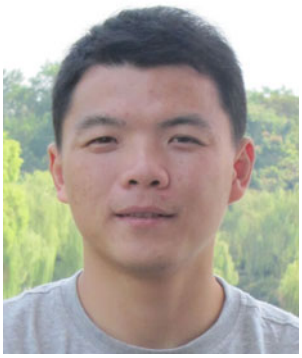

Songjun Zhang received his B.E. degree in science at Xi'an Jiaotong University, China in 2005. He is currently pursuing the Ph.D. degree in science at Xi'an Jiaotong University, China. His research interests include wavelet theory and its applications, and image processing.